A 3-D Time-Dependent Green's Function Approach to Modeling Electromagnetic Noise in On-Chip Interconnect Networks

Zeynep Dilli, Neil Goldsman, Akin Akturk
Dept. of Electrical and Computer Eng.,
University of Maryland,
College Park, MD 20742
dilli@eng.umd.edu

George Metze
Laboratory for Physical Sciences,
8050 Greenmead Dr.,
College Park, MD 20742

***Abstract*— We present a methodology for investigating the response of a complex on-chip interconnect network to external and internal noise, through the development of a 3-D solver based on creating a lumped element model of an interconnect network and solving for its impulse responses. Our method exhibits a lower computational cost than SPICE and allows the user the flexibility to work on a wide variety of interconnect network geometries as well as to include as many parasitic effects as desired for the application.**

I. Introduction

We developed a methodology for investigating the response of a complex on-chip interconnect network to external electromagnetic interference or internal noise, modeled by randomly distributed signals injected into and induced on the network. Our 3-D solver uses the network's impulse responses to characterize its full time- and space-varying outputs.

While full-wave electromagnetic solutions have been used to model on-chip interconnect networks [1], [2], these are computationally intensive for such structures on a semiconducting substrate. The wide variations in the significant dimensions such as layer thicknesses, conductivities and dielectric constants require the creation of a complex mesh with associated numerical problems. For a problem like determining which points on a chip are particularly vulnerable to noise coupling, the ability to quickly repeat simulations on a certain network for many input distributions would be advantageous. Our method provides this ability without having to solve for the entire system repeatedly, saving storage and operation counts.

II. Methodology

We model on-chip interconnect networks as lumped element networks comprised of unit cells, following a similar approach to [3]. Possible unit cell "seed"s for a two-metal process are displayed in Figure 1. Equivalent circuits for unit cells and the couplings between them are obtained through methods to be detailed later.

Next, we set up a lumped-element network using our specific interconnect network layout and determine which output nodes are of interest. For instance, the gate of the transistor in a low-noise amplifier could be picked as a particular point of vulnerability. The responses to impulses induced at or injected into likely input points in the network are then calculated. At this step, the full system is solved. These impulse responses are all we need to get the output for any random signal distribution [4]. Repeating this process to obtain the responses to different random input distributions does not require solving for the response of the the full network again.

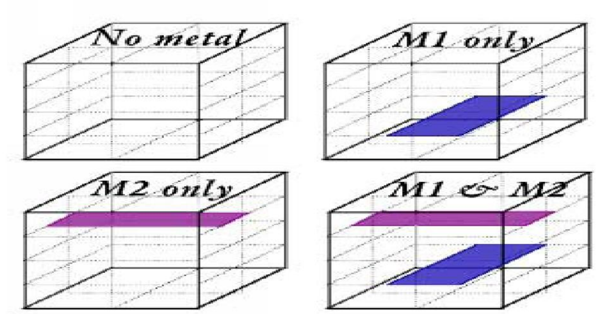

Fig. 1. Unit cell examples for a two-metal process.

This method has two main computational advantages. First, we need to use full-wave solutions only to obtain equivalent circuits for small unit cells if desired. For a preliminary-analysis type approach, a full-wave solution might prove unneeded and unit cells may simply be constructed by inspection.

Second, for selected network points of interest, we need the impulse responses at these points only to have been calculated and stored to get the response to a general input. Especially when exploring effects of random interference, this method has speed and storage advantages over repeating full lumped-network solutions for all possible input distributions.

III. Numerical Modeling

A. Theory

Consider a linear time-invariant system using the spatial coordinate x. Let $h_i[x,t]$ be a system's time-dependent Green's function response at every point in the system to a unit impulse at point x_i and time t=0, $\delta[x-x_i]\delta[t]$:

$$\delta[x-x_i]\delta[t]\longrightarrow h_i[x,t]. \quad (1)$$

We can define an input function $f[x,t]$, whose value at point x_i over all time t is given by

$$f[x_i,t] = f[x,t]\delta[x-x_i]. \quad (2)$$

Sampling this function at time points t_j, we can write it as a summation of impulses marching over time, assuming the time points are sufficiently close and the sampling frequency sufficiently high:

$$f[x_i,t] = \sum_j f[x,t_j]\delta[x-x_i]\delta[t-t_j]. \quad (3)$$

This will then cause the time-dependent system response $F_i[x,t]$ at all points in the system:

$$f[x_i,t] \longrightarrow F_i[x,t] = \sum_j f[x_i,t_j]h_i[x,t-t_j] \ . \quad (4)$$

Thus $F_i[x,t]$ is the contribution to the system response by an input applied at point x_i over the time points t_j. Figure 2 shows two such responses F_1 and F_2 to two inputs f_{i1} and f_{i2}, which are applied at times t_{j1} and t_{j2} respectively.

The principle of superposition [5] gives the response of a linear system to the full input $f[x,t]$ as the sum of all F_i:

$$F[x,t] = \sum_i \sum_j f[x_i,t_j]h_i[x,t-t_j] \quad (5)$$

Thus if the impulse responses $h_i[x_{out},t]$ at point x_{out} to impulses at every possible input point are known, defining a space- and time-dependent random input distribution by the coefficients $\alpha_{i,j} := f[x_i,t_j]$ gives the system output at x_{out} by time-shifting and summation:

$$F[x_{out},t] = \sum_i \sum_j \alpha_{ij}h_i[x_{out},t-t_j] \quad (6)$$

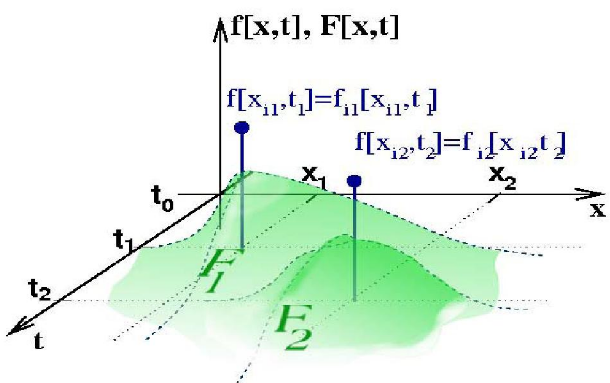

Fig. 2. Time-dependent responses over all space to two individual inputs applied at different x-points at different times t_j.

B. Computational Cost

Once the impulse responses $h_i[x,t]$ have been calculated, to find the response to a time-dependent input $f_i[x,t]$, we proceed by adding the output contribution from each input time step:

$$V_{out}[t] \longleftarrow V_{out}[t] + f_i[t_n] \times h_i[t-t_n] \quad (7)$$

For t_{in} temporal and N_{in} spatial input points, this single multiplication/addition combination is carried out $t_{in}N_{in}t_h$ times, where t_h is the number of timesteps required for the impulse response due to that particular input point to decay. Thus if $t_{in} << t_h$, the operation cost of the time-shifting/summation depends largely on t_h. These scalar-vector multiplications, vector shifting and summations of Eq. 6 are needed only once per input and output points of interest. Assuming there are N_{in} likely input points (e.g. points vulnerable to EM coupling or noise injection as from a power rail) and N_{out} important output points we are interested in, obtaining the entire solution thus requires $N_{in}N_{out}\mathcal{O}(t_h)$ operations.

Repeating the calculation for different random inputs does not require solving the response of the entire network again, whereas SPICE solves the entire network matrix equation at each timestep [6]. Its operation cost per timestep grows as N^m, where N is the number of mesh points and $m > 1$ depends on the matrix equation solution method. Typically, $N >> N_{in}$ or N_{out}, and the number of timesteps depends on how fast the impulse responses decay, paralleling the $\mathcal{O}(t_h)$ component of the cost of our method.

IV. Implementation

Our solver allows convenient construction of large interconnect networks from unit cells. The program has two independent modules: Impulse response solver and input signal response calculator. The former sets up and solves KCL equations for our mesh. The latter performs Eqn. 7 at each output node.

A. Unit Cells and the Lumped Element Network

Possible metal segment combinations in a small area define our unit cells. Various equivalent circuit models, including semiconducting substrate effects, for coupled interconnect segments have been proposed [7], [8]. The element values can be derived by parameter extraction from full-wave simulations or S-parameter measurements [9].

For the purposes of our application, it is critical that the equivalent lumped element network be linear and time-invariant. The common RLCG-type models for single and coupled transmission lines conform to this requirement. For the future expansion of this work, nonlinear loads such as transistor gates may be coupled into certain nodes. The operation conditions should then be assessed carefully to provide a linearized model for such devices.

Figure 3 shows some possible simplified unit cell equivalent circuit definitions in a two-metal technology.

To sum up, combining unit cells with ground connections and on-chip device loads according to the layout, we obtain a full lumped-element network. We can also define unit cells describing the interaction between stacked (3-D) chips' interconnect layers by treating inter-tier vias as analogous to inter-metal layer vias. While the cubic increase in the number of mesh points would limit repeated full analysis of such interconnect networks with SPICE, and although our impulse response calculations are bound by the same limit, once these have been completed finding the full response of a 3-D system to random different inputs with our Green's Function based method is only slightly more complex or computationally intensive than the same operation on a 2-D system.

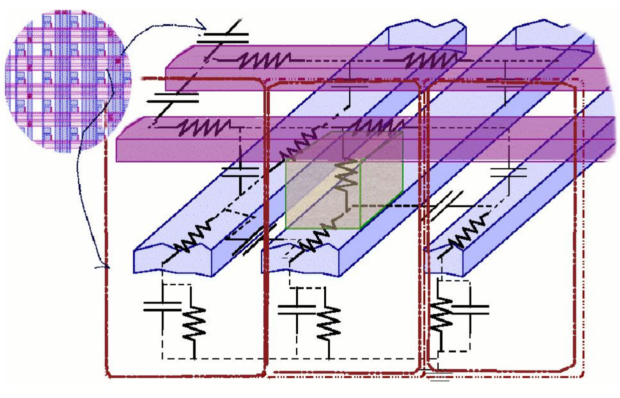

Fig. 3. Two-metal network; a simplified equivalent RC network shown. Possible unit cells partitioned.

B. Sample Results

We have compared both impulse response and full input response solutions with the SPICE results for a 5x5x3 mesh (N=75), in which each node is connected with an R//C to its six nearest neighbours, with bottom layer nodes down-connected to ground and top layer nodes with no up-connections. In this network the north-south resistors are 5 Ω, east-west resistors are 10 Ω, inter-layer resistors are 10 KΩ, and all capacitors are 10 mF. The impulses are injected at points (1,1,1) — bottom layer — and (3,3,2) — middle layer. The full input consists of a 4 ms, 4 A impulse injected at (1,1,1) and 3 ms later a 5 ms, 8 A impulse at (3,3,2); the rise and fall times are 50 μs. Fig. 4 demonstrates the agreement between the SPICE results and our solver. For this mesh, SPICE requires 0.24 msec per timestep, while our input response solver takes 0.0124 msec per timestep and output point. We have performed a convergence analysis on the results of our code to demonstrate that it is first-order convergent, as expected from the time-discretization scheme that was used to set up the KCL equations featuring capacitors.

Figure 5 presents the evolution of an impulse response in time. The larger 21x21x5 system being solved has the same parameters as the 5x5x3 system above. The unit impulse is given at point (1,1,1), at the lowest layer. The figure presents the spread of the Green's function response to this input over 25 ns. At 1 ns the impulse response has reached Layer 5 and begun to spread by coupling between the mesh points. It spreads more in the y-direction, with its smaller resistances, than in the x-direction. At around t=13ns, the peak has decayed considerably and reached the opposite edge, at which point it starts coupling back in the direction it came from. Once again the signal spreads more in the y-direction.

Fig. 6 shows a more complex 50x50x3 (N=7500) network. The two bottom layers are envisioned as bus lines. The top layer is designed after a clock H-tree. Metal 1 (M1) segments are assumed to point north-south (towards the up-right/down-left of the figure) and Metal 2 segments are assumed to point east-west; Metal 3 segments can point either way, depending on where they are in the H-tree.

Between the layers, there is resistive coupling where there are vias and capacitive coupling at other overlapping areas.

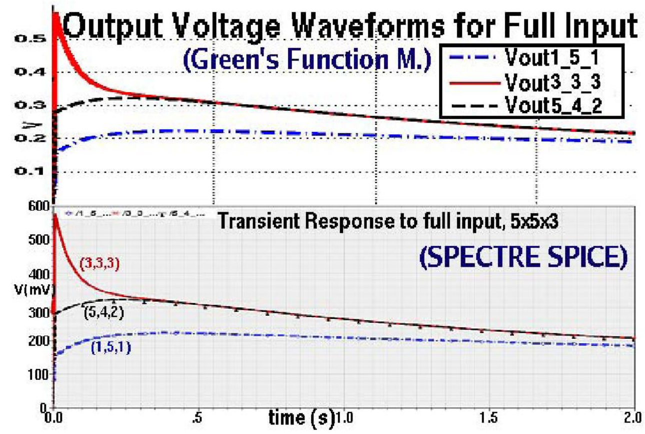

Fig. 4. A 5x5x3 mesh full response simulation. Top: Our solver combines impulse responses at three points using the input data. Bottom: SPICE performs full mesh solution at each timestep for the same input pattern. The solutions match.

At the first level, for points where there are no actual M1 segments, there are still "dummy" nodes where necessary to set up capacitive coupling between the upper metal layers and grounded substrate. There are similar nodes at the second level where such coupling between M1 and M3 layers is needed.

The equivalent lumped element network values were obtained by using experimental data for a three-metal 0.5 μm process, published by the MOSIS fabrication facility [10]. Our network is comprised of 10 μm long, 4 μm wide metal segments, with a 6μm separation.

Fig. 7 shows signals induced at four nodes of this network by a combination of a ground-level, 0.1 mA noise spike injected at (5,15,1), and a top-level, 5 mA interference pulse injected at (25,25,3), the center of the H-tree. The closest output at (29,50,3) has the highest response to the (25,25,3) input; it is worth noting that the other three, equidistant points however exhibit different responses to this input thanks to the effects of the lower metal layers and a via on the path to (9,1,3). The lower left point (9,1,3) is found to be most sensitive to the ground-level pulse due to proximity and the presence of a close resistive path. The different end points of the H-network respond with different time constants and sensitivities to this input. With our method it is easy to explore the location-dependent response to other input signals.

V. Conclusion

A computationally efficient method for the analysis of noise coupling to on-chip interconnect networks is presented. We solve for the impulse responses of a lumped element network created by defining interconnect unit cells and extracting their equivalent circuit parameters, which reflect the semiconducting substrate and geometric effects of the layout. We can adapt the method for 2-D or 3-D systems by changing the coupling networks between unit cells, which might model layers in a chip stack. Thereafter the effects of different inputs can be obtained simply from these impulse responses without having to solve for the full network. Thus the method allows rapid exploration of the responses of different layouts to many different inputs.

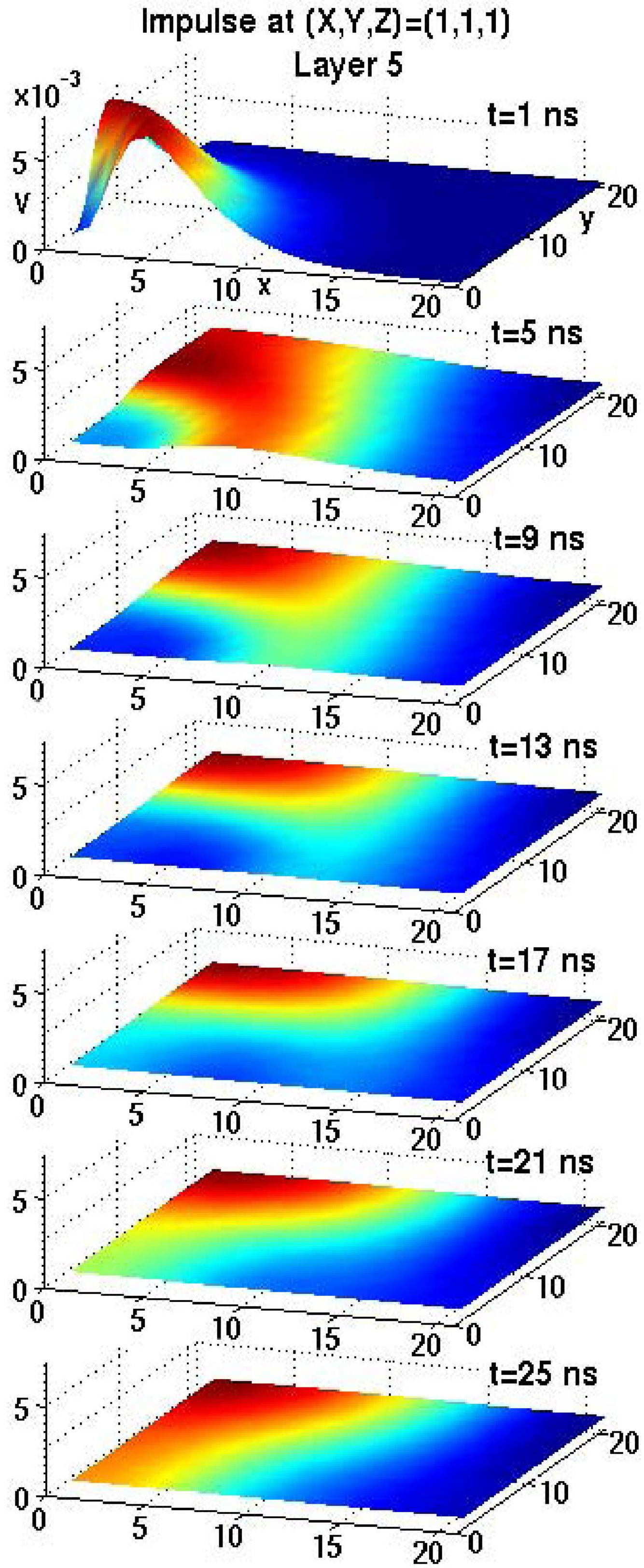

Fig. 5. The time evolution of the Green's Function of a 21x21x5 system on the topmost level, i.e. layer 5. The unit impulse was injected at time t=0 at point (1,1,1): The lower left corner of the lowest level, layer 1. The response spreads unevenly since the north-south resistivity of this network is smaller than the east-west resistivity.

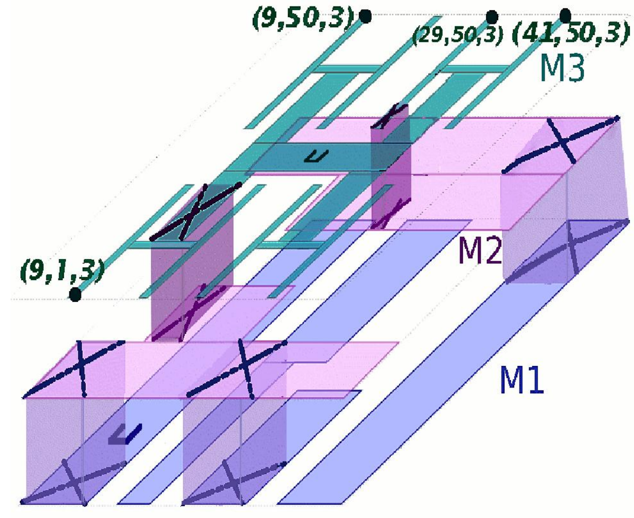

Fig. 6. 3-metal interconnect network. Vias:**X**. Inputs: ⊔.Outputs: •.

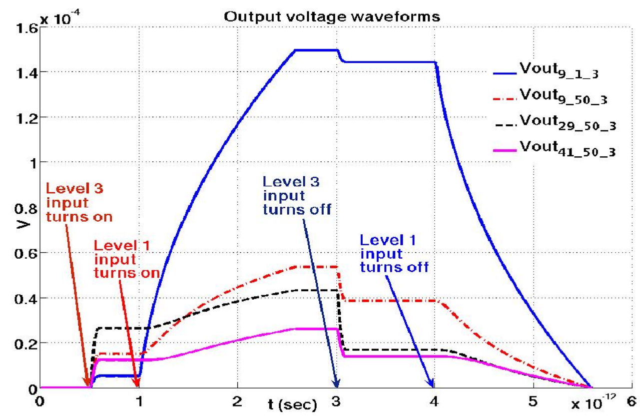

Fig. 7. Responses of the network in Fig.6 to a combined input signal injected at points (5,15,1) and (25,25,3). Distance as well as the effect of inter-level coupling and presence of paths to ground affect the responses.

Acknowledgment

The authors would like to thank Bo Yang for invaluable discussions.

References

[1] Meuris, P., Schoenmaker, W., *IEEE Tr. on Computer-Aided Des. of Int. Cir. and Syst.*, v.20, no.6, pp. 753-762.
[2] Shao, X.,Goldsman, N., Ramahi, O., Guzdar, P., International Conf. on Sim. of Semicond. Proc. and Dev. (SISPAD)'03, pp. 315-317.
[3] Akturk, A., Goldsman, N., Parker, L., Metze, G., *Solid-State Elec.*, v.49, pp.1125-1134, 2005.
[4] Dilli, Z., Goldsman, N., Akturk. A., International Symp. on Semicond. Dev. Res. (ISDRS) '05.
[5] Oppenheim, A.V., Willsky, A.S., Young, I.T. *Signals and Systems,* Prentice Hall, USA, 1983.
[6] http://www.ecircuitcenter.com/SpiceTopics/Overview/Overview.htm, visited in Feb. 2006.
[7] Zheng, J., Hahm, Y.-C., Tripathi, V.K., Weisshaar, A., *IEEE Tr. on Mic. Th. and Tech.*, v.48, no.9, pp. 1443-1451.
[8] Weisshaar, A., Lan, H., Luoh, A., *IEEE Tr. on Adv. Pack.*, v.25, no.2, pp. 288-296.
[9] Jiao, D., Mazumder, M., Chakravarty, S., Dai, C., Kobrinsky, M.J., Harmes, M.C., List, S., SISPAD'03, pp. 39-42.
[10] http://www.mosis.org/Technical/Testdata/ami-c5-prm.html, visited in June 2006.

